BMC Pulmonary Medicine

RESEARCH

Open Access

A novel chronic obstructive pulmonary disease mouse model induced by intubation-mediated intratracheal co-administration of porcine pancreatic elastase and lipopolysaccharide

Won-Yong Shim[1], Sun-Min Seo[1], Dong-Hyun Kim[1], Young-Jun Park[1], Na-Won Kim[1], Eun-Seon Yoo[1], Ji-Hun Lee[1], Han-Bi Jeong[1], Jin-Hee Seo[2], Kyoung-Sun Lee[3] and Yang-Kyu Choi[1,4*]

Abstract

Background Chronic obstructive pulmonary disease (COPD) is a significant respiratory disorder in humans characterized by persistent airway constriction or obstruction due to chronic bronchitis and pulmonary emphysema. Various methods of inducing COPD in mouse models are frequently used in COPD research; however, these cannot completely reproduce histopathologic lesions. This study aimed to establish a new COPD mouse model that reproduces histopathological lesions closely resembling clinical COPD within a shorter induction time.

Methods The new strategy involved the co-administration of porcine pancreatic elastase (PPE) and lipopolysaccharide (LPS), with PPE intended to induce pulmonary emphysema and LPS intended to induce chronic bronchitis. Male C57BL/6J mice were administered PPE (8 U/kg) on days 0 and 3 and LPS (400 μg/kg) on days 6, 9, 12, and 15. Each administration was performed using a noninvasive intubation-mediated intratracheal instillation method with a laryngoscope.

Results Postmortem examination on day 22 revealed that pulmonary emphysema and chronic bronchitis were simultaneously induced in 90.91% of the lung lobes. Molecular studies revealed higher messenger ribonucleic acid (mRNA) expression levels of interleukin-6(IL-6) and matrix metalloproteinase-12(MMP-12) associated with the pathogenesis of COPD.

Conclusion A new method was developed to establish a COPD mouse model that displays a more severe representation of the histopathological findings of clinical COPD than previous COPD models. It also reduces the time required for model induction. This newly developed COPD mouse model is expected to be a valuable tool for the pathogenesis and therapeutic research on human COPD.

*Correspondence:
Yang-Kyu Choi
yangkyuc@konkuk.ac.kr

Full list of author information is available at the end of the article

Keywords Chronic obstructive pulmonary disease, Porcine pancreatic elastase, Lipopolysaccharide, Pulmonary emphysema, Chronic bronchitis

Background

Chronic obstructive pulmonary disease (COPD) is a chronic inflammatory condition characterized by persistent airway constriction that results in breathing difficulties during daily activities. The primary cause of COPD is long-term exposure to cigarette smoke (CS); however, it can also develop in individuals exposed to environmental air pollutants and workplace dust. COPD presents two distinct pathological conditions: 'chronic bronchitis,' characterized by persistent inflammation of the bronchi and airway obstruction, and 'emphysema,' which involves the loss of alveolar wall elasticity, leading to increased alveolar volume and difficulties in gas exchange. These conditions can also cause acute exacerbations owing to infection. COPD is an irreversible disease that involves progressive damage to the lung parenchyma and can lead to the deterioration of lung function, weight loss, pneumothorax, and even death if unmanaged [1]. As of 2019, COPD was the third leading cause of death globally [2].

Three main methods are mostly used to induce COPD in mice to investigate its etiology, prevention, and treatment: chronic exposure to CS, respiratory administration of porcine pancreatic elastase (PPE), and respiratory administration of lipopolysaccharide (LPS) [3, 4]. Given that smoking is the primary cause of COPD in humans, CS exposure allows the creation of mouse models that can most closely mimic the etiological conditions of human COPD. However, CS exposure protocols are limited because they are not standardized, cannot replicate severe lesions, and require a prolonged period of at least six months for disease induction [3, 5].

PPE instillation is frequently used when creating animal models of pulmonary emphysema. When introduced into the lungs of mice, PPE degrades the elastic fibers of the alveolar walls, causing pulmonary emphysema within 3–4 weeks [6–9]. However, this model replicates only one aspect of COPD pathology and has etiological differences from actual human COPD [5, 10]. LPS administration in mouse models induces acute lung injury, simulating acute exacerbations in patients with clinical COPD [11, 12]. However, it is restricted to reproducing some elements of COPD pathogenesis and misses significant features, such as chronic bronchitis and pulmonary emphysema [13, 14]. Some models employ extended, low-dose LPS exposure to more accurately mimic the pathological features of COPD, requiring a substantial induction period of at least 8–12 weeks [15, 16].

Although these approaches offer specific advantages, they may present drawbacks, including time-demanding protocols, inability to reproduce histopathological lesions, and etiological disparities from clinical COPD. Therefore, this study aimed to develop a novel mouse model of COPD by sequentially administering PPE and LPS to induce emphysema and chronic bronchitis, thus replicating a similar model of progressive COPD in humans within a shorter induction time.

Methods

Animals

Male C57BL/6J mice were purchased from DBL (Chungbuk, Republic of Korea) and maintained at the College of Veterinary Medicine, Konkuk University. The animal housing facility was maintained at a temperature of 22±2 °C, a humidity of 50±10%, and a 12-h light-dark cycle. The Institutional Animal Care and Use Committee at Konkuk University, Seoul, Republic of Korea, approved all animal use and care protocols (KU23078).

PPE and LPS

Elastase from porcine pancreas (PPE, E1250, Sigma-Aldrich, USA), with a concentration of 6.9 mg protein/mL and enzymatic activity of 6 units/mg protein, was stored in light-protected containers at 4 °C. Before administration, PPE was diluted with sterilized normal saline. LPS powder (LPS, L2630, Sigma-Aldrich, USA) was dissolved in sterilized saline at a 2 mg/mL concentration and maintained at -20 °C. The solution was thawed before each use, and a solution that had been thawed once was not reused.

Intubation-mediated intratracheal instillation

In this study, the modified intubation-mediated intratracheal instillation method was employed to precisely administer agents into the lower respiratory tract [17]. Initially, mice were anesthetized with a combination of Zoletil® 50 (tiletamine+zolazepam) at a dose of 20 mg/kg and Rompun® (xylazine HCl) at 5 mg/kg via the intraperitoneal route (10 mL/kg). The equipment for intubation and instillation included a mouse intubation stand, a laryngoscope for mice, a 22 G intravenous catheter, curved forceps, a 1 mL syringe, a 100 µL pipette, a 70-mm rubber band, and a Catgut suture. The anesthetized mice were placed on an intubation stand. The tracheal entrance was exposed using a mouse-specific laryngoscope, and a 22-G intravenous catheter was inserted through the vocal cords for intubation. Following intubation, 50 µL of the agent was administered using a pipette and a 1 mL syringe. To ensure even distribution of the agents, we initiated the administration immediately after passing the vocal folds to a point sufficiently before the

bifurcation of the trachea and rapidly injected over 100 µL of air immediately after the administration. Additionally, we administered agents with the trachea intubated in a manner that kept the delivery as parallel to the airway lumen as possible. Furthermore, after each administration, the mice were positioned in different axis positions to promote a more uniform distribution across the lung lobes. The mice were monitored until they regained respiration and consciousness.

Experimental design

Male C57BL/6J mice were divided into the normal control (NC), PPE, LPS, and PPE/LPS groups. The NC group received 50 µL of normal saline on days 0, 3, 6, 9, 12, and 15 (n=10). The PPE group received 8 U/kg PPE on days 0 and 3 (n=10). The LPS group received 400 µg/kg of LPS on days 6, 9, 12, and 15 (n=10). The PPE/LPS group received PPE (8 U/kg) on days 0 and 3, followed by LPS (400 µg/kg) on days 6, 9, 12, and 15 (n=16). Each instillation was performed using the intubation-mediated intratracheal instillation technique. The body weights of mice were measured once daily. After the final administration, mice in all groups were allowed a 7-day recovery period. A postmortem examination was performed on day 22. A comprehensive schematic of the experimental design is shown in Fig. 1.

Necropsy

Mice were anesthetized with 5% isoflurane in an anesthetic chamber and maintained with 3% isoflurane through a gas mask. After confirming the absence of deep pain using a toe pinch, euthanasia was performed by exsanguination of the caudal vena cava. Subsequently, the thoracic cavity was gently exposed to avoid lung injury, and all the lung lobes were excised from the beginning of the airway. For some individuals in each group, the remaining lobes were stored in a deep freezer for molecular analysis.

Hematoxylin and eosin (H&E) staining

Following the postmortem examination, the collected lungs were adequately inflated with a 10% formalin solution and fixed for 24 h. After fixation, tissue-processing procedures involving dehydration, clearing, and infiltration were performed. The processed tissues were embedded into paraffin blocks and cut into 4 µm-thick slides. These slides underwent H&E staining.

Histopathological evaluation

Various parameters related to air spaces within the lung lobes were measured using a light microscope (Olympus, Japan). First, the air/tissue (AT) ratio was determined to represent the proportion of air in the entire lung lobe. Second, the emphysema lesion area within the lung lobe section, indicating regions with significantly enlarged alveoli and thinner alveolar walls, was measured.

The inflammatory site/lobar area, which quantified the number of areas with ≥50 aggregated inflammatory cells per 1 mm^2 lung section, was determined to evaluate the severity of chronic bronchitis. Emphysema was considered present in a lung lobe if even some emphysema lesions were found, while chronic bronchitis was considered present if the inflammatory site/lobar area was 1.0 or more. If emphysema and chronic bronchitis were simultaneously present within a single lung lobe, a COPD lesion was considered. Based on these criteria, the induction rate, representing the success rate of lesion induction, was assessed for each lobe in the PPE/LPS model group. Additionally, the histopathological parameters for each lobe were analyzed to evaluate the consistency

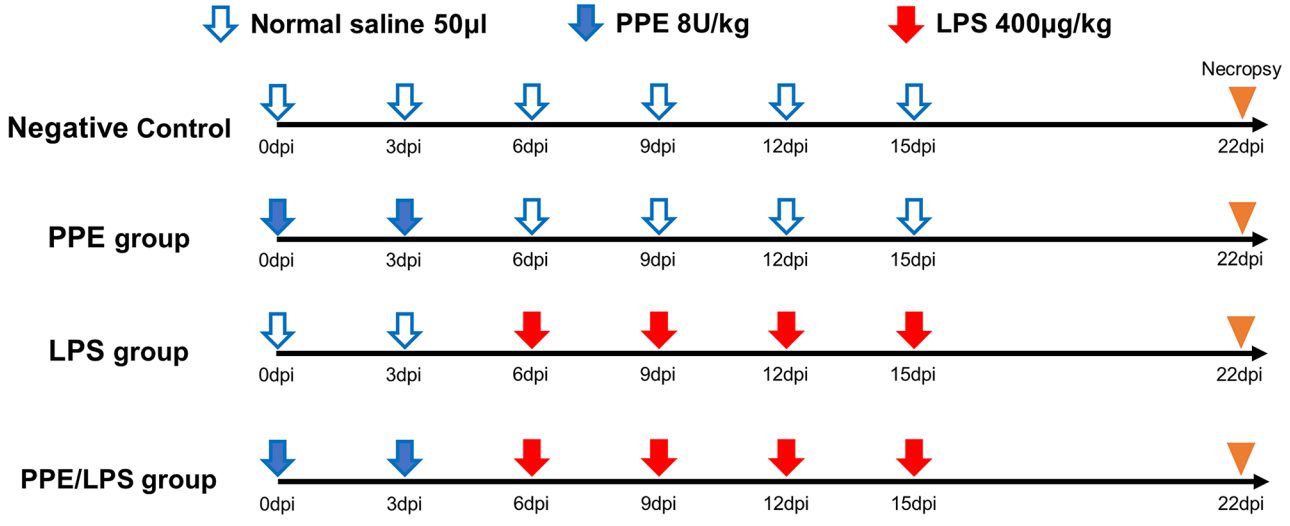

Fig. 1 Experimental design of animal studies. Mice were divided into the normal control (n=10), PPE (n=10), LPS (n=10), and PPE/LPS (n=16) groups

Table 1 List of primer sequences for quantitative polymerase chain reaction

Gene	Sequence (5′-3′)	
	Forward	Reverse
GAPDH	AACTTTGGCATTGTGGAAGG	ACACATTGGGGGTAGGAACA
IL-6	ACAAGTCGGAGGCTTAATTACACAT	TTGCCATTGCACAACTCTTTTC
MMP-12	TGAGGCAGAAACGTGGACTAAA	ATTGACTTTGGATTATTGGAATGCT
IL-1α	ACGGCTGAGTTTCAGTGAGACC	CACTCTGGTAGGTGTAAGGTGC
IL-1β	TGGACCTTCCAGGATGAGGACA	GTTCATCTCGGAGCCTGTAGTG
MMP-9	TCTTCCCCAAAGACCTGAAAAC	GCCCGGGTGTAACCATAGC
IL-13	AACGGCAGCATGGTATGGAGTG	TGGGTCCTGTAGATGGCATTGC
TNF-α	AGGCTGCCCCGACTACGT	GACTTTCTCCTGGTATGAGATAGCAAA
IFN-γ	GCCTGCTGGTGGTAAAGAAACTGA	ATCAGGGTGGAGGAGCAGTGGCGGC

of histopathological lesion induction among the five lung lobes in the PPE/LPS model group.

Each lung lobe was photographed at a magnification of ×12.5, resulting in images with a resolution of 5,760×3,600 pixels, using OLYMPUS cellSens Standard software (Olympus, USA). The AT ratio and lung lobe area were subsequently analyzed using Metamorph software (BioVision Technologies, USA). First, area of each lung lobe was measured by analyzing the cross sections of lung lobes. Then, the air-filled regions within the lobes were identified and marked. To calculate the AT ratio, the area of air-filled region was divided by the total lobe area.

RNA extraction

The frozen left lung lobe was homogenized using 500 µL of RD buffer from the MagListo™ 5 M Universal RNA Extraction Kit (K-3613, BIONEER, Republic of Korea) in the FastPrep-24™ 5G bead beating system (116005500, MP Biomedicals, USA). Subsequently, approximately 100 µL of RNA solution was obtained following the protocol of the MagListo™ 5 M Universal RNA Extraction Kit. The total RNA concentration was measured using the NanoDrop™ 1000 (Thermo Fisher, USA).

Quantitative polymerase chain reaction (qPCR)

RNA (1 µg) was added to Maxime™ RT PreMix (Oligo(dT)15 Primer) (25081, iNtRON Biotechnology, Republic of Korea) for complementrary deoxyribonucleic acid (cDNA) synthesis. The mixture was adjusted to a volume of 20 µL with sterile distilled water, and cDNA synthesis was performed using T100™ Thermal Cycler (BIO-RAD, USA) with a protocol of 45 °C for 60 min followed by 95 °C for 5 min. For quantitative PCR, the CFX96™ Touch Real-Time PCR Detection System (BIO-RAD, USA) was used, including 10 µL of AccuPower® GreenStar™ RT-qPCR Master Mix (K-6403, BIONEER, Republic of Korea), 7 µL of diethyl pyrocarbonate (DEPC)-treated water, 1 µL of cDNA, forward primer (10 pmol), and reverse primer (10 pmol). Glyceraldehyde-3-phosphate dehydrogenase (GAPDH) was selected as the housekeeping gene to measure the relative mRNA expression levels. The relative mRNA expression levels of COPD-related molecules, including interleukin (IL)-6, matrix metalloproteinase (MMP)-12, IL-1α, IL-β, MMP-9, IL-13, tumor necrosis factor-α (TNF-α), and interferon-γ (IFN-γ), were quantified. The nucleotide sequences of the primers used in the experiments are listed in Table 1 [18].

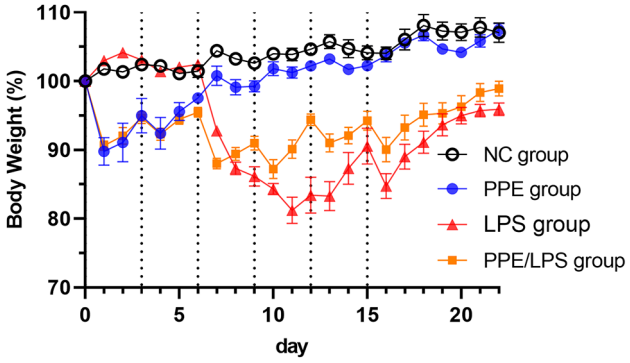

Fig. 2 Body weight changes. The body weight of all mice in each group was measured daily for 22 days. Body weights were presented as a percentage of their initial weights. The dotted lines along the X-axis indicate the days of PPE or LPS administration. The graphs include the mean weight changes and standard error ($n=10$ for NC, $n=5$ for PPE, $n=10$ for LPS, $n=16$ for PPE/LPS group)

Statistical analysis

Statistical analysis was conducted using GraphPad Prism 9.0 (GraphPad Software Inc., USA), and the P-values obtained through one-way analysis of variance (ANOVA) and Tukey's multiple comparison tests were interpreted as follows: $^{*}P<0.05$, $^{**}P<0.01$, $^{***}P<0.001$.

Results

Change in body weight following PPE and LPS administration

Consistent decreases in body weight were observed on the day following the agent administration, followed by recovery within 2–3 days (Fig. 2). During the 7-day recovery period following the last administration, weight restoration was 107% in the PPE group, 96% in the LPS group, and 99% in the PPE/LPS group. Table 2

Table 2 Detailed body weight data by timepoints of agent administration (unit = body weight of the day / initial body weight × 100%)

Group / Timepoint	Day 0	Day 3	Day 6	Day 9	Day 12	Day 15	Day 22
NC group	100.00	102.41	101.46	102.61	104.65	104.13	107.05
PPE group	100.00	95.00	97.56	99.23	102.22	102.24	107.50
LPS group	100.00	103.10	102.41	86.16	83.42	90.54	95.91
PPE/LPS group	100.00	94.69	95.48	90.97	94.39	94.26	98.93

Co-administration of PPE and LPS simultaneously induced emphysema and chronic bronchitis

Consistent histopathological features were observed on the cross-sectional lung slides in each group. In the NC group, no inflammatory cells were observed around the bronchi, and the alveolar size was normal (Fig. 3A and B). In the PPE group, a significantly enlarged alveolar appearance was evident throughout the lung lobes, indicating emphysema (Fig. 3C and D). In the LPS group, chronic inflammatory cells, such as lymphocytes, monocytes, and macrophages, infiltrated the bronchi, bronchioles, and blood vessels, manifesting as characteristic lesions of chronic bronchitis in multiple locations (Fig. 3E and F). Notably, in the PPE/LPS group, the distinctive histopathological features of COPD, including emphysema and chronic bronchitis, were concurrently observed in a single lung lobe (Fig. 3G and H).

The average AT ratio in the NC and LPS groups was 0.58 and 0.59, respectively. In contrast, the PPE and PPE/LPS groups showed significantly increased AT ratios (0.84 and 0.81, respectively) (Fig. 4A). This result demonstrates an AT ratio increase of >40% with PPE administration. The emphysema areas were 53.5% and 58.64% in the PPE and PPE/LPS groups, respectively (Fig. 4B). The inflammatory site/lobar area was 1.89/mm^2 and 1.88/mm^2 in the LPS and PPE/LPS groups, respectively (Fig. 4C). In the PPE group, the inflammatory site/lobar area was 0.34/mm^2, indicating relatively mild bronchitis.

Homogeneous distribution of histopathologic lesions in all pulmonary lobes

The AT ratio in the PPE/LPS group ranged from 0.76 in the accessory lobe, with the highest value observed in the right cranial lobe at 0.95; however, there were no statistically significant differences among the five lobes (Fig. 4D). The emphysema area was the lowest in the right middle lobe (46.09%) and the highest in the right cranial lobe (70.31%). The inflammatory site/lobar area was the lowest in the right caudal lobe (1.49/mm^2) and the highest in the accessory lobe (2.24/mm^2) (Fig. 4E). Nevertheless, there were no statistically significant differences in histopathological parameters between the lobes.

Regarding the distribution of histopathological parameters in the PPE/LPS group, a minimum induction rate of 93.75% was achieved in the right middle and right caudal lobes. The right cranial lobe had a minimum induction rate of 81.25% for chronic bronchitis, indicating a high overall success rate. In the left lobe, the induction rates of pulmonary emphysema and chronic bronchitis were 100%. The lesion induction rates in the five lobes demonstrated a high prevalence of emphysema (98.18%) and chronic bronchitis (94.55%). Simultaneous induction of pulmonary emphysema and chronic bronchitis was observed in 90.91% of all lung lobes (Fig. 4F).

Co-administration of PPE and LPS induced various biochemical conditions of COPD

The relative expression of IL-6 was significantly increased in the PPE/LPS group compared to that in the NC group, amounting to a 9.1-fold increase. The differences between the PPE/LPS and PPE groups and the PPE/LPS and LPS groups were 4.36-fold and 6.03-fold, respectively (Fig. 5A). Additionally, the relative expression of MMP-12 significantly increased by 39.8-fold in the PPE/LPS group compared to that in the NC group. Comparison with the PPE and LPS groups revealed 4.50-fold and 4.26-fold increases, respectively (Fig. 5B). For other molecules, the mRNA expression of IL-1α exhibited a statistically significant increase in the PPE/LPS group (Fig. 5C), while the mRNA expression of IL-1β, MMP-9, and IL-13 exhibited a statistically significant decrease in the PPE/LPS group compared to the NC group (Fig. 5D-F). No statistically significant differences in TNF-α and IFN-γ expression were observed between the NC and model groups (Fig. 5G and H).

Discussion

Although various mouse models are available for COPD research, they cannot simultaneously induce the histopathological hallmarks of severe chronic bronchitis and pulmonary emphysema, which are crucial features of clinical COPD [5]. This study introduced a novel method to overcome the limitations of the existing COPD mouse models. This method involves the induction of emphysema through intratracheal instillation of PPE, followed by repetitive LPS administration to induce chronic bronchitis. Histopathological lesions resembling actual COPD were successfully induced within a significantly shorter period of 22 days. In addition, various parameters were used to assess the histopathological lesions to evaluate the adequacy of the model for investigating COPD.

In body weight change analysis, we observed that animals regained their body weight within approximately three days after the administration of disease-inducing

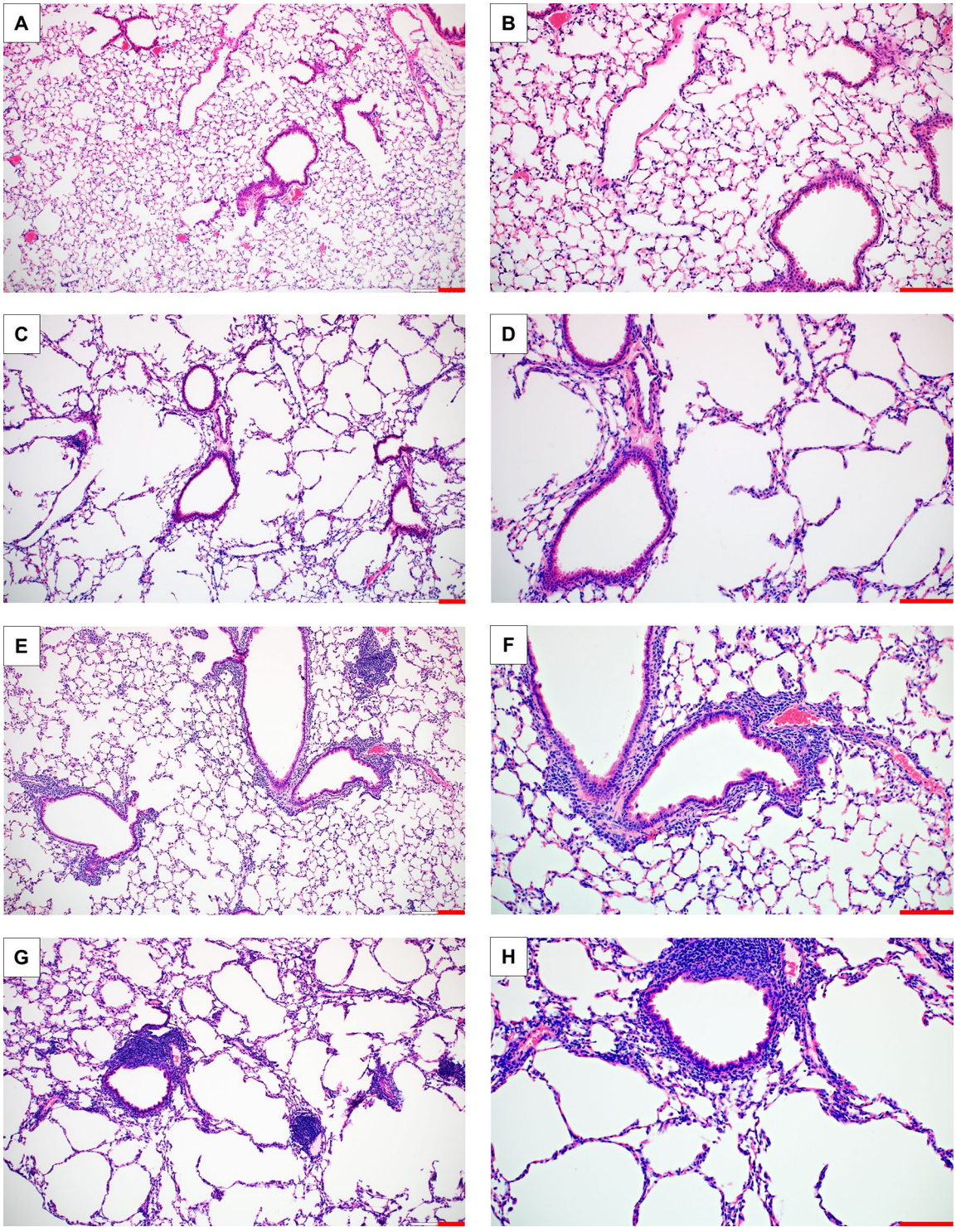

Fig. 3 Histopathological features. The representative images of the lung from the four groups exhibit bronchioles and surrounding alveolars. (**A**, **B**) Lung section of the normal control group. (**C**, **D**) Lung section of PPE group. (**E**, **F**) Lung section of LPS group. (**G**, **H**) Lung section of PPE/LPS group. Red scale bar = 100 μm

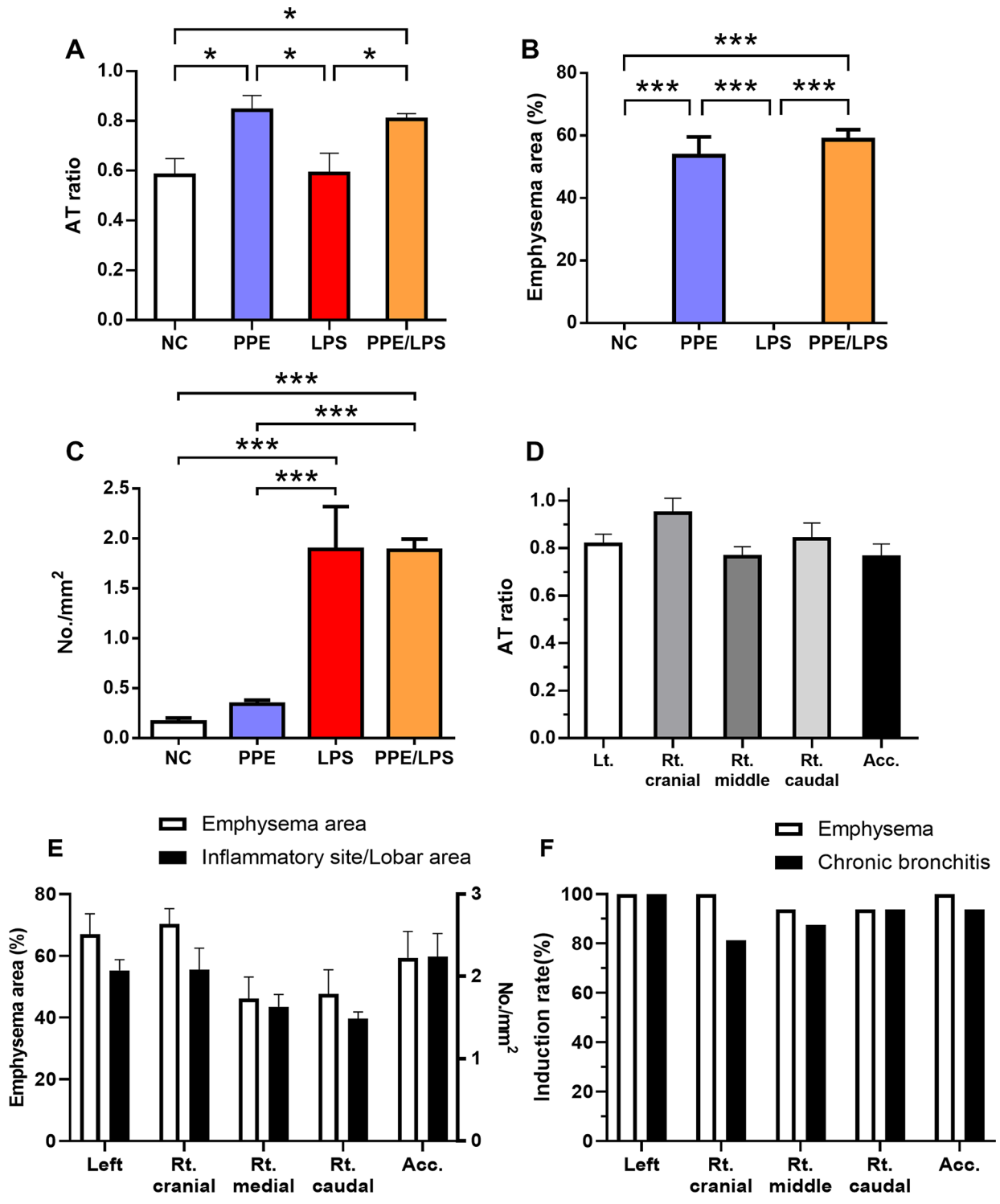

Fig. 4 Histopathological parameters and distribution of histopathologic lesions. (**A**) Air/tissue ratio of each group. (**B**) Emphysema area of each group. (**C**) Inflammatory site/lobar area of each group. (**D**) Air/tissue ratio of each lobe in the PPE/LPS group. (**E**) Emphysema area and inflammatory site/lobar area of each lobe in the PPE/LPS group. (**F**) Lesion induction rate of each of five lung lobes in the PPE/LPS group. The graphs include the mean parameters and standard error. *$P < 0.05$, **$P < 0.01$, ***$P < 0.001$ as assessed using one-way ANOVA and Tukey's multiple comparisons test ($n = 5$ for NC, $n = 5$ for PPE, $n = 4$ for LPS, $n = 11$ for PPE/LPS group)

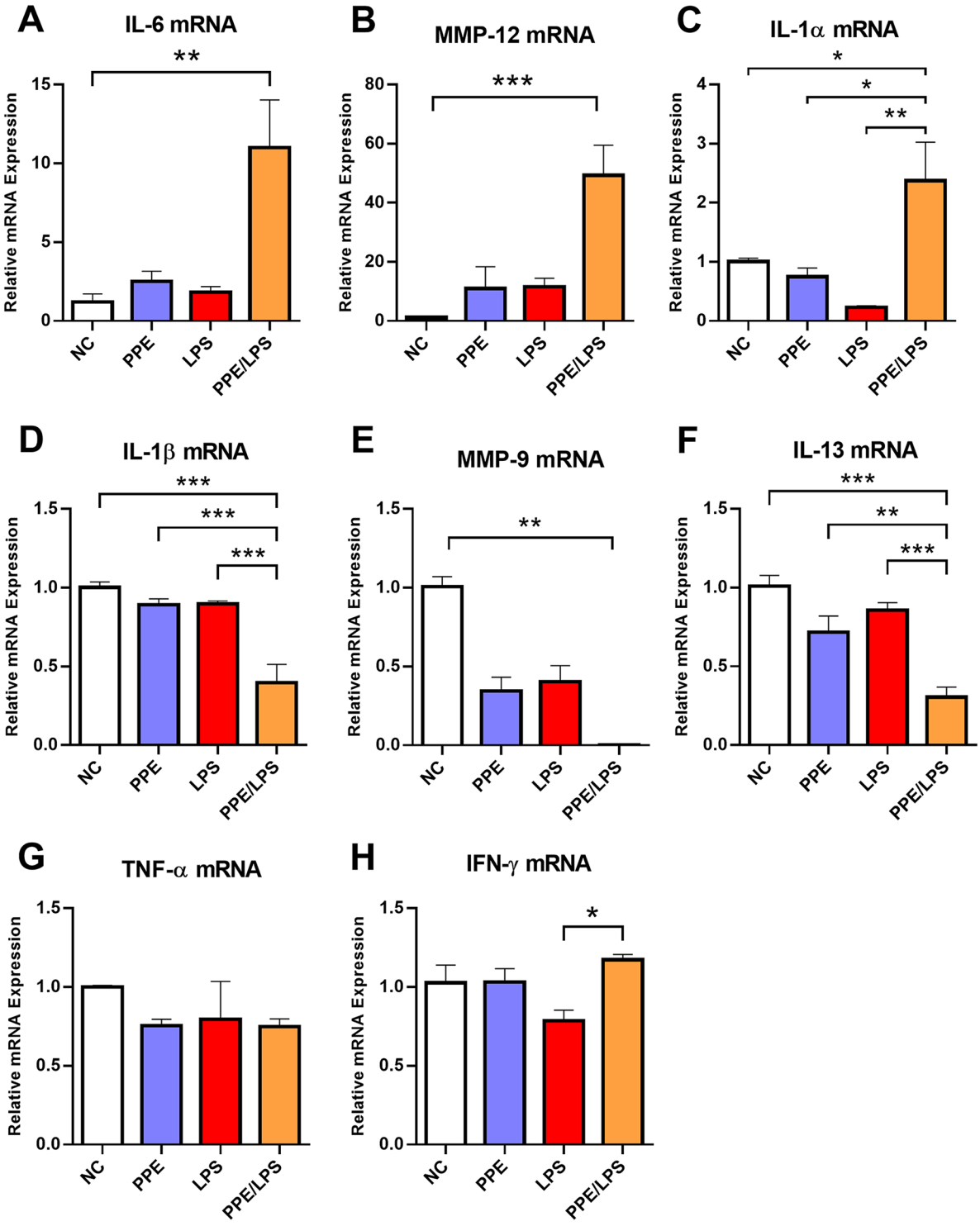

Fig. 5 Relative mRNA expression of molecules. The relative mRNA expression levels, compared to GAPDH, are represented in the graphs for each group. (**A**) Relative mRNA expression of IL-6. (**B**) Relative mRNA expression of MMP-12. (**C**) Relative mRNA expression of IL-1α. (**D**) Relative mRNA expression of IL-1β. (**E**) Relative mRNA expression of MMP-9. (**F**) Relative mRNA expression of IL-13. (**G**) Relative mRNA expression of TNF-α. (**H**) Relative mRNA expression of IFN-γ. The graphs include the mean parameters and standard error. *$P < 0.05$, **$P < 0.01$, ***$P < 0.001$ as assessed using one-way ANOVA and Tukey's multiple comparisons test ($n = 5$ per group)

agents. Based on these preliminary findings, we established a three-day interval for substance administration in our model. By the end of the study, the body weight of animals in the model group was lower than that of the NC group, which we interpreted as a reduction in weight gain due to the chronic nature of the disease induced by the model.

Regarding the evaluation methods used in this study, two parameters were employed to assess pulmonary emphysema induction in the lung lobes: the AT ratio and the extent of the emphysema lesion area. Many COPD researchers use the mean linear intercept (MLI) to measure the severity of emphysema induced in mouse lung lobes, depending solely on the MLI for evaluation, which has several limitations [19–21]. In the PPE-induced model, achieving uniform levels of emphysema throughout the entire lung lobes is challenging because of the solution-based delivery of the substance. This is because of the difficulty in achieving homogeneity in lesions within the same lung lobe and the time-consuming nature of manual measurements [22]. Moreover, the MLI may not fully capture changes in the air space in a three-dimensional context [23, 24]. Therefore, the AT ratio was introduced in this study to achieve a more uniform evaluation of emphysema in lung lobes [25–27]. The significant increase in the AT ratio in the groups that received PPE demonstrates the effectiveness of this parameter as an evaluation criterion. Additionally, the AT ratio evaluation, conducted using the Metamorph® program, offers a simpler and faster assessment, making it a more appropriate method for histopathological analysis in the new COPD mouse model rather than the labor-intensive MLI measurements.

As histopathological analysis can assess only a single cross-section of lung tissue in a two-dimensional manner, there is the potential for overlooking histopathologic lesions when emphysema induction is insufficient. Therefore, an additional analysis based on the extent of emphysema induced within the lung lobe was performed to measure how much PPE affects the lung tissue when delivered into the lung lobe. The significantly high emphysema area in the PPE-treated groups suggests that two repeated administrations of PPE at 8 U/kg each induced a substantial degree of emphysema, affecting at least 50% of the alveoli in a single lung lobe and ensuring that the lesions were sufficiently prominent.

The severity of chronic bronchitis was assessed using histopathological analysis based on the number of inflammatory sites per lobar area. The markedly elevated number of inflammatory sites in the LPS and PPE/LPS groups demonstrate that repetitive LPS administration induces the aggregation of chronic inflammatory cells surpassing 1.5 aggregates per 1 mm^2 of the lung lobe. This finding indicates that a four-fold repeated LPS administration at 400 μg/kg can sufficiently induce a relatively more severe chronic inflammation in a shorter time than the previous CS-induced model [28]. Following the previously referenced study, we observed more than 6 lymphoid aggregates in our model compared to the observation of 1 or fewer in the conventional CS model under 200x magnification, indicating a significantly higher severity of inflammation. By contrast, the PPE group exhibited fewer inflammatory sites, indicating mild inflammation. This observation may be associated with the regenerative processes triggered by PPE-induced damage, which can lead to a mild inflammatory response [13].

In developing COPD models in mice, uniform disease induction across all five lung lobes is crucial because human COPD is not confined to specific lobes but manifests across multiple lung lobes [29]. This is particularly significant when conducting histopathological and molecular studies within the same mouse, as inconsistent distributions can lead to notable discrepancies in the results. Additionally, the uniformity in the distribution of emphysematous changes correlates with the severity of airway obstruction in patients [51]. To achieve a consistent distribution of lesions throughout all lung lobes, we established a refined repetitive intubation-mediated intratracheal administration method instead of intranasal administration. This approach minimizes agent loss due to nasal structures and eliminates its impact on the nasal epithelium, while also ensuring uniform lesion distribution. Evaluation of lesion distribution within the model group showed sufficiently consistent induction of pulmonary emphysema and chronic bronchitis across all lobes. In addition, 90.91% of all lung lobes displayed both histopathological lesions, confirming the successful induction of COPD. These results emphasize the consistency and reliability of this model for the histopathological analysis of any selected lobe.

The molecular mechanisms associated with the induction and exacerbation of COPD involve a complex interaction of diverse inflammatory pathways, making it challenging to designate any single pathway as the primary cause of the disease [4, 30, 31]. Considering this, several key molecules involved in COPD-related pathways were selected. Among them, IL-6, IL-1α, and MMP-12 exhibited significant increases in mRNA expression in the PPE/LPS group. IL-6, known for its role in fibrosis by promoting myofibroblast proliferation, has been linked to COPD [32]. Moreover, circulating IL-6 has been recognized as a promising diagnostic biomarker for COPD [33, 34]. The significant increase in IL-6 levels in the new model reinforces its potential as a diagnostic biomarker for COPD. Moreover, the precise role of IL-1α in the disease pathogenesis of asthma and COPD has been demonstrated [35]. In our study, the marked increase in the expression levels of IL-6 and IL-1α mRNA suggests that

the biochemical context observed in the CS-induced mouse model was reproduced in the new model [36, 37].

MMP-12 is well-established for its central role in alveolar destruction and COPD induction in mouse models [38, 39]. MMP-12 functions as both a direct protease and a pro-inflammatory factor, making it a critical parameter for assessing the severity of COPD and a therapeutic target for COPD treatment [40–46]. In the present study, a remarkable elevation in MMP-12 expression in the PPE/LPS group aligns with recent research emphasizing the essential role of MMP-12 in emphysema development in a PPE-induced mouse model [47]. The significant difference in the mRNA expression levels underscores its potential as a valuable evaluation parameter, further supporting MMP-12 as a promising therapeutic target for future applications in this model. These results indicate the overexpression of pro-inflammatory cytokines and proteases resulting from the combined administration of PPE and LPS in the model group, suggesting that sustained pulmonary damage may be attributed to the autoimmunity of these molecules [48].

TNF-α and IFN-γ were anticipated to be relevant molecules associated with COPD [18]. However, our results did not show statistically significant differences in the expression levels of these molecules between the test and control groups. This lack of significant induction suggests that while TNF-α and IFN-γ are important in COPD, their expression may not be markedly altered in the current model under the conditions tested. Potential reasons for this include compensatory mechanisms that might be masking changes in these cytokines, as well as temporal dynamics where the expression levels of TNF-α and IFN-γ might not align with the specific time points or stages assessed in our study.

The new COPD mouse model introduced in this study differs slightly in its induction mechanisms from those of actual COPD. The main pathogenic mechanism in human COPD is an imbalance of proteases and anti-proteases due to chronic stimulation, leading to the persistent remodeling of pulmonary structures [4]. However, in the PPE-induced COPD model, emphysema is initiated by an externally introduced substance rather than by endogenous factors, which is recognized as a key limitation of this model [13]. Nevertheless, the crucial point is that this model can more rapidly induce histopathological features resembling actual COPD compared to the previous CS-induced COPD model. In addition, the severity of COPD lesions is more marked than in the CS-induced model [49]. This results in more dramatic lesions, which are easier to evaluate through histopathological analysis. The clarity in lesion severity may enhance the precision and ease of evaluating treatment efficacy by clearly demonstrating differences between control and treated groups. 'Additionally, it is known that centralilobular emphysema in COPD patients can indeed lead to significant symptomatic and physiological consequences [50]. Specifically, central emphysematous change may affect pulmonary function compared to peripheral emphysema [51]. Building upon this insight, we speculate that our model, which may induces emphysema lesions in central region through the administration of liquid-form inducing agents, could potentially lead to a more pronounced manifestation of COPD. Consequently, this model is anticipated to be more suitable for research related to the maintenance and treatment of COPD rather than the prevention or therapies for early-stage COPD. Despite the differences in induction mechanisms, several studies have been conducted on valuable therapeutic research using the PPE-induced COPD mouse model [48, 52]. Moreover, as most patients with COPD receive medical care after the disease has already progressed chronically and generally require lifelong management, the focus in COPD research is now shifting toward maintenance and therapeutic research rather than prevention [53].

Co-administering PPE and LPS is not the first attempt to overcome the limitations of COPD induction methods; however, previous approaches lacked standardization [25, 54]. While existing co-administration methods deliver inducing agents via the intranasal route, our method introduces noninvasive intratracheal instillation for more precise substance delivery. In addition, this new method significantly reduces the induction period compared to existing methods, which ranges from 31 days to 20 weeks. Furthermore, this study analyzed the severity of lesions, the induced areas of lesions within the pulmonary lobes, and the distribution of lesions across the lung lobes. This comprehensive analysis enhances the potential for consistent reproducibility in future studies on COPD mouse models.

One major limitation of our COPD model is the absence of obstructive changes, which is a key characteristic of human COPD. This limitation is a common issue in small animal models due to the anatomical differences between rodents and humans [14]. In particular, rodents have fewer mucus-producing goblet cells and more non-ciliated epithelial cells, which make it difficult to replicate mucus hypersecretion and subsequent airway obstruction. While we were unable to fully replicate obstructive changes, we were able to successfully reproduced several hallmark features of COPD, providing a valuable platform for studying key aspects of the disease and its progression. Additionally, the lack of pulmonary function tests in our study further limits the ability to comprehensively evaluate airway obstruction and hinders a more in-depth comparison with other COPD models.

Although we conducted various histopathological and biochemical evaluations of the novel model, further studies are required to determine the optimal timing for drug

administration. Additionally, other distinct evaluative parameters, such as serum biochemical parameters and pulmonary function, are needed for a more detailed analysis of COPD progression.

Conclusions

This study demonstrated the effectiveness of a newly developed COPD mouse model created via the co-administration of PPE and LPS. This novel model is significant for inducing histopathological features similar to those of clinical COPD within a shorter induction time compared to previous CS-induced COPD mouse models. Considering the relative severity of the induced histopathological lesions in this model, it is appropriate to investigate the progression, exacerbation, maintenance, and treatment of COPD.

Abbreviations

AT	Air/tissue
COPD	Chronic obstructive pulmonary disease
CS	Cigarette smoke
IL	Interleukin
LPS	Lipopolysaccharide
MLI	Mean linear intercept
MMP	Matrix metalloproteinase
NC	Normal control
PPE	Porcine pancreatic elastase

Supplementary Information

The online version contains supplementary material available at https://doi.org/10.1186/s12890-024-03365-3.

Supplementary Material 1: Supplementary information 1. Changes in body weights and pathology analysis data from all experiments, including preliminary studies, Supplementary information 2. Data used for building graphs and the original graph data, Supplementary information 3. Supplementary figures of each group.

Acknowledgements

We would like to thank Editage (www.editage.co.kr) for English language editing.

Author contributions

Conceptualization: Shim WY, Seo JH, Lee KS, Choi YK. Formal analysis: Shim WY, Seo SM. Funding acquisition: Choi YK. Investigation: Shim WY, Kim NW, Yoo ES, Jeong HB. Methodology: Shim WY, Kim DH, Park YJ, Lee JH. Project administration: Seo SM, Choi YK. Supervision: Choi YK. Writing – original draft: Shim WY. Writing – review & editing: Seo JH, Lee KS, Choi YK. All authors read and approved the final manuscript.

Funding

This work was supported by the National Research Foundation of Korea (NRF) grant funded by the Korea government (MSIT) (2021M3H9A1030260 and 2021M3H9A1097269). The funders had no role in study design, data collection and analysis, decision to publish, or preparation of the manuscript.

Data availability

All data generated or analysed during this study are included in this published article.

Declarations

Ethics approval and consent to participate

This study was conducted following the ARRIVE guidelines. This study obtained approval from the Institutional Animal Care and Use Committee at Konkuk University, Seoul, Republic of Korea, for all experimental animal usage and procedures, with approval number KU23078. All animal experiments were performed under anesthesia to minimize suffering to the mice.

Consent for publication

Not applicable.

Competing interests

The authors declare no competing interests.

Author details

[1]Department of Laboratory Animal Medicine, College of Veterinary Medicine, Konkuk University, Seoul 05029, Republic of Korea
[2]Korea Radioisotope Center for Pharmaceuticals, Korea Institute of Radiological & Medical Sciences, Seoul 01812, Republic of Korea
[3]Non-Clinical Evaluation Center, Osong Medical Innovation Foundation, Cheongju 28160, Republic of Korea
[4]KU Center for Animal Blood Medical Science, Konkuk University, Seoul 05029, Republic of Korea

Received: 24 July 2024 / Accepted: 25 October 2024
Published online: 12 November 2024

References

1. Robert AW, Chronic Obstructive Pulmonary Disease (COPD). Sep 2022 [Cited 23 Oct 2023]. In: MSD MANUAL Professional Version [Internet]. https://www.msdmanuals.com/en-kr/professional/pulmonary-disorders/chronic-obstructive-pulmonary-disease-and-related-disorders/chronic-obstructive-pulmonary-disease-copd#v914610
2. Alison B, Andrei M. WHO reveals leading causes of death and disability worldwide: 2000–2019. 9 Dec 2020 [Cited 2 Oct 2023]. In: World Health Organization [Internet]. https://www.who.int/news/item/09-12-2020-who-reveals-leading-causes-of-death-and-disability-worldwide-2000-2019
3. Ghorani V, Boskabady MH, Khazdair MR, Kianmeher M. Experimental animal models for COPD: a methodological review. Tob Induc Dis. 2017;15:1–13. https://doi.org/10.1186/s12971-017-0130-2.
4. Tanner L, Single AB. Animal models reflecting chronic obstructive pulmonary disease and related respiratory disorders: translating pre-clinical data into clinical relevance. J Innate Immun. 2020;12(3):203–25. https://doi.org/10.1159/000502489.
5. Bonfield TL. In vivo models of lung disease. Lung diseases-selected state of the art Reviews, InTech. 2012;407 – 28.
6. Joshi I, Devine AJ, Joshi R, Smith NJ, Varisco BM. A titratable murine model of progressive emphysema using tracheal porcine pancreatic elastase. Sci Rep. 2023;13(1):15259. https://doi.org/10.1038/s41598-023-41527-1.
7. Oliveira MV, Abreu SC, Padilha GA, Rocha NN, Maia LA, Takiya CM, et al. Characterization of a mouse model of emphysema induced by multiple instillations of low-dose elastase. Front Physiol. 2016;7:457. https://doi.org/10.3389/fphys.2016.00457.
8. Shimoyama T, Kaneda M, Yoshida S, Michihara S, Fujita N, Han LK, et al. Ninjin'yoeito ameliorated PPE-induced pulmonary emphysema and anxiety/depressive-like behavior in aged C57BL/6J mice. Front Pharmacol. 2022;13:970697. https://doi.org/10.3389/fphys.2016.00457.
9. Fysikopoulos A, Seimetz M, Hadzic S, Knoepp F, Wu CY, Malkmus K, et al. Amelioration of elastase-induced lung emphysema and reversal of pulmonary hypertension by pharmacological iNOS inhibition in mice. Br J Pharmacol. 2021;178(1):152–71. https://doi.org/10.1111/bph.15057.
10. Suki B, Bartolák-Suki E, Rocco P. Elastase-induced lung emphysema models in mice. Alpha-1 Antitrypsin Deficiency: Methods Protocols. 2017;67–75. https://doi.org/10.1007/978-1-4939-7163-3_7.
11. Tsikis ST, Fligor SC, Hirsch TI, Pan A, Yu LJ, Kishikawa H, et al. Lipopolysaccharide-induced murine lung injury results in long-term pulmonary changes and downregulation of angiogenic pathways. Sci Rep. 2022;12(1):10245. https://doi.org/10.1038/s41598-022-14618-8.

12. Roos AB, Berg T, Ahlgren KM, Grunewald J, Nord M. A method for generating pulmonary neutrophilia using aerosolized lipopolysaccharide. JoVE (Journal Visualized Experiments). 2014;94e51470. https://doi.org/10.3791/51470.
13. Chow L, Smith D, Chokshi K, Ezegbunam W, Charoenpong P, Foley K, et al. Animal models of Chronic Obstructive Pulmonary. COPD: Update Pathogenesis Clin Manage. 2018;1. https://doi.org/10.5772/intechopen.70262.
14. Wright JL, Cosio M, Churg A. Animal models of chronic obstructive pulmonary disease. Am J Physiology-lung Cell Mol Physiol. 2018;295(1):L1–15. https://doi.org/10.1152/ajplung.90200.2008.
15. Vernooy JH, Dentener MA, Van Suylen RJ, Buurman WA, Wouters EF. Long-term intratracheal lipopolysaccharide exposure in mice results in chronic lung inflammation and persistent pathology. Am J Respir Cell Mol Biol. 2002;26(1):152–9. https://doi.org/10.1165/ajrcmb.26.1.4652.
16. Brass DM, Hollingsworth JW, Cinque M, Li Z, Potts E, Toloza E, et al. Chronic LPS inhalation causes emphysema-like changes in mouse lung that are associated with apoptosis. Am J Respir Cell Mol Biol. 2008;39(5):584–90. https://doi.org/10.1165/rcmb.2007-0448OC.
17. Lawrenz MB, Fodah RA, Gutierrez MG, Warawa J. Intubation-mediated intratracheal (IMIT) instillation: a noninvasive, lung-specific delivery system. JoVE (Journal Visualized Experiments). 2014;93e52261. https://doi.org/10.3791/52261.
18. Eurlings IM, Dentener MA, Mercken EM, de Cabo R, Bracke KR, Vernooy JH. A comparative study of matrix remodeling in chronic models for COPD; mechanistic insights into the role of TNF-α. Am J Physiology-Lung Cell Mol Physiol. 2014;307(7):L557–65. https://doi.org/10.1152%2Fajplung.00116.2014.
19. Munoz-Barrutia A, Ceresa M, Artaechevarria X, Montuenga LM, Ortiz-de-Solorzano C. Quantification of lung damage in an elastase-induced mouse model of emphysema. J Biomedical Imaging. 2012;5–5. https://doi.org/10.1155/2012/734734.
20. Crowley G, Kwon S, Caraher EJ, Haider SH, Lam R, Batra P, et al. Quantitative lung morphology: semi-automated measurement of mean linear intercept. BMC Pulm Med. 2019;19:1–9. https://doi.org/10.1186/s12890-019-0915-6.
21. Salsabili S, Lithopoulos M, Sreeraman S, Vadivel A, Thébaud B, Chan AD, et al. Fully automated estimation of the mean linear intercept in histopathology images of mouse lung tissue. J Med Imaging. 2021;8(2):027501–027501. https://doi.org/10.1117/1.JMI.8.2.027501.
22. Nakashima R, Kamei S, Nohara H, Fujikawa H, Maruta K, Kawakami T, et al. Auto-measure emphysematous parameters and pathophysiological gene expression profiles in experimental mouse models of acute and chronic obstructive pulmonary diseases. J Pharmacol Sci. 2019;140(2):113–9. https://doi.org/10.1016/j.jphs.2019.01.011.
23. Knudsen L, Weibel ER, Gundersen HJG, Weinstein FV, Ochs M. Assessment of air space size characteristics by intercept (chord) measurement: an accurate and efficient stereological approach. J Appl Physiol. 2010;108(2):412–21. https://doi.org/10.1152/japplphysiol.01100.2009.
24. Weibel ER, Hsia CC, Ochs M. How much is there really? Why stereology is essential in lung morphometry. J Appl Physiol. 2007;102(1):459–67. https://doi.org/10.1152/japplphysiol.00808.2006.
25. Khedoe PPSJ, Wong MC, Wagenaar GT, Plomp JJ, van Eck M, Havekes LM, et al. The effect of PPE-induced emphysema and chronic LPS-induced pulmonary inflammation on atherosclerosis development in APOE* 3-LEIDEN mice. PLoS ONE. 2013;8(11):e80196. https://doi.org/10.1371/journal.pone.0080196.
26. Redente EF, Kopf KW, Bahadur AN, Robichaud A, Lundblad LK, McDonald LT. Application-specific approaches to MicroCT for evaluation of mouse models of pulmonary disease. PLoS ONE. 2023;18(2):e0281452. https://doi.org/10.1371/journal.pone.0281452.
27. Khalajzeyqami Z, Grandi A, Ferrini E, Ravanetti F, Leo L, Mambrini M, et al. Pivotal role of micro-CT technology in setting up an optimized lung fibrosis mouse model for drug screening. PLoS ONE. 2022;17(6):e0270005. https://doi.org/10.1371/journal.pone.0270005.
28. Serré J, Tanjeko AT, Mathyssen C, Vanherwegen AS, Heigl T, Janssen R, et al. Enhanced lung inflammatory response in whole-body compared to nose-only cigarette smoke-exposed mice. Respir Res. 2021;22:1–15. https://doi.org/10.1186/s12931-021-01680-5.
29. Emam M, de la Faverie JR, Gharbi N, El-Gohary MI. Characterization of lung's emphysema distribution: Numerical assessment of disease development. In 4th International Conference on New Trends in Information Science and Service Science. 2010;pp. 464–469. IEEE.
30. Wang C, Zhou J, Wang J, Li S, Fukunaga A, Yodoi J, Tian H. Progress in the mechanism and targeted drug therapy for COPD. Signal Transduct Target Therapy. 2020;5(1):248. https://doi.org/10.1038/s41392-020-00345-x.
31. Boucherat O, Morissette MC, Provencher S, Bonnet S, Maltais F. Bridging lung development with chronic obstructive pulmonary disease. Relevance of developmental pathways in chronic obstructive pulmonary disease pathogenesis. Am J Respir Crit Care Med. 2016;193(4):362–75. https://doi.org/10.1164/rccm.201508-1518PP.
32. Chung KF. Cytokines in chronic obstructive pulmonary disease. Eur Respir J. 2001;18. https://doi.org/10.1183/09031936.01.00229701. :34 Suppl 50s-59s.
33. Bradford E, Jacobson S, Varasteh J, Comellas AP, Woodruff P, O'Neal W, et al. The value of blood cytokines and chemokines in assessing COPD. Respir Res. 2017;18(1):1–11. https://doi.org/10.1186/s12931-017-0662-2.
34. Agusti A, Sin DD. Biomarkers in COPD. Clin Chest Med. 2014;35(1):131–41. https://doi.org/10.1016/j.ccm.2013.09.006.
35. Osei ET, Brandsma CA, Timens W, Heijink IH, Hackett TL. Current perspectives on the role of interleukin-1 signalling in the pathogenesis of asthma and COPD. Eur Respir J. 2020;55(2). https://doi.org/10.1183/13993003.00563-2019.
36. Botelho FM, Bauer CM, Finch D, Nikota JK, Zavitz CC, Kelly A, et al. IL-1α/IL-1R1 expression in chronic obstructive pulmonary disease and mechanistic relevance to smoke-induced neutrophilia in mice. PLoS ONE. 2011;6(12):e28457. https://doi.org/10.1371/journal.pone.0028457.
37. Yang Y, Di T, Zhang Z, Liu J, Fu C, Wu Y, et al. Dynamic evolution of emphysema and airway remodeling in two mouse models of COPD. BMC Pulm Med. 2021;21(1):1–10. https://doi.org/10.1186/s12890-021-01456-z.
38. Christopoulou ME, Papakonstantinou E, Stolz D. Matrix metalloproteinases in Chronic Obstructive Pulmonary Disease. Int J Mol Sci. 2023;24(4):3786. https://doi.org/10.3390/ijms24043786.
39. Gharib SA, Manicone AM, Parks WC. Matrix metalloproteinases in emphysema. Matrix Biol. 2018;73:34–51. https://doi.org/10.1016/j.matbio.2018.01.018.
40. Churg A, Zhou S, Wright JL. Matrix metalloproteinases in COPD. Eur Respir J. 2012;39(1):197–209. https://doi.org/10.1183/09031936.00121611.
41. Le Quement C, Guenon I, Gillon JY, Valenca S, Cayron-Elizondo V, Lagente V, et al. The selective MMP-12 inhibitor, AS111793 reduces airway inflammation in mice exposed to cigarette smoke. Br J Pharmacol. 2008;154(6):1206–15. https://doi.org/10.1038/bjp.2008.180.
42. Baggio C, Velazquez JV, Fragai M, Nordgren TM, Pellecchia M. Therapeutic targeting of MMP-12 for the treatment of chronic obstructive pulmonary disease. J Med Chem. 2020;63(21):12911–20. https://doi.org/10.1021/acs.jmedchem.0c01285.
43. Molet S, Belleguic C, Lena H, Germain N, Bertrand CP, Shapiro SD, et al. Increase in macrophage elastase (MMP-12) in lungs from patients with chronic obstructive pulmonary disease. Inflamm Res. 2005;54:31–6. https://doi.org/10.1007/s00011-004-1319-4.
44. Demedts IK, Morel-Montero A, Lebecque S, Pacheco Y, Cataldo D, Joos GF, et al. Elevated MMP-12 protein levels in induced sputum from patients with COPD. Thorax. 2006;61(3):196–201. https://doi.org/10.1136/thx.2005.042432.
45. Hunninghake GM, Cho MH, Tesfaigzi Y, Soto-Quiros ME, Avila L, Lasky-Su J, et al. MMP12, lung function, and COPD in high-risk populations. N Engl J Med. 2009;361(27):2599–608. https://doi.org/10.1056/NEJMoa0904006.
46. Haq I, Chappell S, Johnson SR, Lotya J, Daly L, Morgan K, et al. Association of MMP-12 polymorphisms with severe and very severe COPD: a case control study of MMPs-1, 9 and 12in a European population. BMC Med Genet. 2010;11(1):1–11. https://doi.org/10.1186/1471-2350-11-7.
47. Shibata S, Miyake K, Tateishi T, Yoshikawa S, Yamanishi Y, Miyazaki Y, et al. Basophils trigger emphysema development in a murine model of COPD through IL-4–mediated generation of MMP-12–producing macrophages. Proc Natl Acad Sci. 2018;115(51):13057–62. https://doi.org/10.1073/pnas.1813927115.
48. Takeda K, Kim SH, Joetham A, Petrache I, Gelfand EW. Therapeutic benefits of recombinant alpha1-antitrypsin IgG1 Fc-fusion protein in experimental emphysema. Respir Res. 2021;22:1–11. https://doi.org/10.1186/s12931-021-01784-y.
49. Sasaki M, Chubachi S, Kameyama N, Sato M, Haraguchi M, Miyazaki M, et al. Evaluation of cigarette smoke-induced emphysema in mice using quantitative micro-computed tomography. Am J Physiology-Lung Cell Mol Physiol. 2015;308(10):L1039–45. https://doi.org/10.1152/ajplung.00366.2014.
50. Smith BM, Austin JH, Newell JD Jr, D'Souza BM, Rozenshtein A, Hoffman EA, et al. Pulmonary emphysema subtypes on computed tomography: the MESA COPD study. Am J Med. 2014;127(1):94–e7. https://doi.org/10.1016/j.amjmed.2013.09.020.
51. Haraguchi M, Shimura S, Hida W, Shirato K. Pulmonary function and regional distribution of emphysema as determined by high-resolution computed tomography. Respiration. 1998;65(2):125–9. https://doi.org/10.1159/000029243.

52. Massaro GDC, Massaro D. Retinoic acid treatment abrogates elastase-induced pulmonary emphysema in rats. Nat Med. 1997;3(6):675–7. https://doi.org/10.1038/nm0697-675.
53. Kostikas K, Price D, Gutzwiller FS, Jones B, Loefroth E, Clemens A, et al. Clinical impact and healthcare resource utilization associated with early versus late COPD diagnosis in patients from UK CPRD database. Int J Chronic Obstr Pulm Dis. 2020;1729–38. https://doi.org/10.2147/COPD.S255414.
54. Sajjan U, Ganesan S, Comstock AT, Shim J, Wang Q, Nagarkar DR, et al. Elastase-and LPS-exposed mice display altered responses to rhinovirus infection. Am J Physiology-Lung Cell Mol Physiol. 2009;297(5):L931–44. https://doi.org/10.1152/ajplung.00150.2009.

Publisher's note